JCI The Journal of Clinical Investigation

A phosphotyrosine switch determines the antitumor activity of ERβ

Bin Yuan, … , Qinong Ye, Rong Li

J Clin Invest. 2014;124(8):3378-3390. https://doi.org/10.1172/JCI74085.

Research Article **Oncology**

Estrogen receptors ERα and ERβ share considerable sequence homology yet exert opposite effects on breast cancer cell proliferation. While the proliferative role of ERα in breast tumors is well characterized, it is not clear whether the antitumor activity of ERβ can be mobilized in breast cancer cells. Here, we have shown that phosphorylation of a tyrosine residue (Y36) present in ERβ, but not in ERα, dictates ERβ-specific activation of transcription and is required for ERβ-dependent inhibition of cancer cell growth in culture and in murine xenografts. Additionally, the c-ABL tyrosine kinase and EYA2 phosphatase directly and diametrically controlled the phosphorylation status of Y36 and subsequent ERβ function. A nonphosphorylatable, transcriptionally active ERβ mutant retained antitumor activity but circumvented control by upstream regulators. Phosphorylation of Y36 was required for ERβ-mediated coactivator recruitment to ERβ target promoters. In human breast cancer samples, elevated phosphorylation of Y36 in ERβ correlated with high levels of c-ABL but low EYA2 levels. Furthermore, compared with total ERβ, the presence of phosphorylated Y36–specific ERβ was strongly associated with both disease-free and overall survival in patients with stage II and III disease. Together, these data identify a signaling circuitry that regulates ERβ-specific antitumor activity and has potential as both a prognostic tool and a molecular target for cancer therapy.

Find the latest version:

https://jci.me/74085/pdf

A phosphotyrosine switch determines the antitumor activity of ERβ

Bin Yuan,[1,2,3] Long Cheng,[1] Huai-Chin Chiang,[3] Xiaojie Xu,[1] Yongjian Han,[1] Hang Su,[4] Lingxue Wang,[1] Bo Zhang,[5] Jing Lin,[6] Xiaobing Li,[5] Xiangyang Xie,[1] Tao Wang,[7] Rajeshwar R. Tekmal,[8] Tyler J. Curiel,[9] Zhi-Min Yuan,[4] Richard Elledge,[9] Yanfen Hu,[3] Qinong Ye,[1,2] and Rong Li[3]

[1]Department of Medical Molecular Biology, Beijing Institute of Biotechnology, Collaborative Innovation Center for Cancer Medicine, Beijing, China. [2]Institute of Cancer Stem Cell, Cancer Center, Dalian Medical University, Liaoning, China. [3]Department of Molecular Medicine and [4]Department of Radiation Oncology, University of Texas Health Science Center at San Antonio, San Antonio, Texas, USA. [5]Department of Pathology, Affiliated Hospital of Academy of Military Medical Sciences Beijing, China. [6]First Affiliated Hospital, Chinese PLA General Hospital, Beijing, China. [7]Department of Breast Cancer, Affiliated Hospital of Academy of Military Medical Sciences, Beijing, China. [8]Department of Obstetrics and Gynecology and [9]Department of Medicine, University of Texas Health Science Center at San Antonio, San Antonio, Texas, USA.

Estrogen receptors ERα and ERβ share considerable sequence homology yet exert opposite effects on breast cancer cell proliferation. While the proliferative role of ERα in breast tumors is well characterized, it is not clear whether the antitumor activity of ERβ can be mobilized in breast cancer cells. Here, we have shown that phosphorylation of a tyrosine residue (Y36) present in ERβ, but not in ERα, dictates ERβ-specific activation of transcription and is required for ERβ-dependent inhibition of cancer cell growth in culture and in murine xenografts. Additionally, the c-ABL tyrosine kinase and EYA2 phosphatase directly and diametrically controlled the phosphorylation status of Y36 and subsequent ERβ function. A nonphosphorylatable, transcriptionally active ERβ mutant retained antitumor activity but circumvented control by upstream regulators. Phosphorylation of Y36 was required for ERβ-mediated coactivator recruitment to ERβ target promoters. In human breast cancer samples, elevated phosphorylation of Y36 in ERβ correlated with high levels of c-ABL but low EYA2 levels. Furthermore, compared with total ERβ, the presence of phosphorylated Y36–specific ERβ was strongly associated with both disease-free and overall survival in patients with stage II and III disease. Together, these data identify a signaling circuitry that regulates ERβ-specific antitumor activity and has potential as both a prognostic tool and a molecular target for cancer therapy.

Introduction

The 2 estrogen receptors ERα and ERβ mediate diverse effects of estrogens in multiple tissues (1). Despite considerable sequence homology, ERα and ERβ carry out nonredundant physiological functions. While ERα is critical for mediating estrogen-dependent proliferation during normal mammary gland development, ERβ is known to inhibit cell proliferation and promote differentiation in a number of tissues (1, 2). In cancer development and progression, ERα has a well-established role in supporting estrogen-dependent breast tumor growth, whereas ERβ significantly attenuates cell proliferation and invasion in a number of cancer cell types including breast (3–6) and prostate cancers (7–9). Lower expression of ERβ is found in breast cancer and correlates with worse disease outcome (10). The fact that ERβ is still present in a large percentage of breast tumors raises the possibility of mobilizing the antitumor activity of ERβ as a potential therapy (11). However, this opportunity has not been extensively exploited, partly due to the paucity of knowledge about how such ERβ activity can be harnessed in tumor cells.

Mammalian eye absent (EYA) proteins are involved in cell-fate determination in a broad spectrum of cells and tissues (12). EYA proteins are transcription coregulators with well-documented tyrosine phosphatase activity (13–15). The phosphatase activity of EYA is important for its roles in transcriptional regulation (14, 16), cytoplasmic signaling (17), innate immune response (18), and DNA damage–induced apoptosis (19, 20). The oncogenic activity of EYA proteins has been demonstrated in ovarian (21) and breast cancers (22, 23). In particular, EYA2 was shown to promote proliferation, migration, and invasion of breast cancer cells, but its direct target(s) in tumor promotion is unclear.

The oncogenic activity of BCR-ABL due to chromosomal translocation in chronic myelogenous leukemia (CML) has been extensively investigated (24), and pharmacological inhibition of the c-ABL kinase activity represents one of the most successful rationale design–based cancer therapies (25). However, the function of native c-ABL protein in solid tumor development remains controversial (26). In the case of breast cancer, c-ABL was reported to promote survival and motility of breast cancer cells (27, 28). On the other hand, c-ABL was shown to mediate the tumor-suppressor activity of EPHB4 (29) and inhibit oncogenic transforming growth factor-β signaling (30) in breast tumorigenesis. Furthermore, recent clinical trials of c-ABL antagonists for several solid tumor types, including breast cancer, yielded mixed results (31, 32).

Authorship note: Bin Yuan and Long Cheng contributed equally to this work.
Conflict of interest: The authors have declared that no conflict of interest exists.
Submitted: November 5, 2013; **Accepted:** May 1, 2014.
Reference information: *J Clin Invest*. 2014;124(8):3378–3390. doi:10.1172/JCI74085.

Therefore, the exact role of c-ABL in cancer development and progression is likely to be context dependent.

In the current study, we sought to elucidate the mechanism by which ERβ-specific function is regulated in breast cancer cells. We identified a phosphotyrosine residue (Y36) present in ERβ, but not in ERα, that is critical for ERβ-specific transcriptional and antitumor activities. Our work also led to the discovery of c-ABL and EYA2 as the kinase and phosphatase, respectively, that regulate the antitumor activity of ERβ by directly controlling the phosphorylation status of Y36.

Results

EYA2 modulates transcriptional activity of ERβ, not ERα. To identify proteins that specifically regulate ERβ but not ERα, we used ERβ AF1 (amino acid 1-148), the region most divergent from ERα, as the bait in a yeast 2-hybrid screen. We isolated EYA2 from the initial screen and verified its association with ERβ by coimmunoprecipitation (co-IP) of endogenous EYA2 and ERβ in MCF7 breast cancer cells (Figure 1A) and glutathione-S-transferase pulldown of recombinant proteins (Figure 1B). The EYA2-ERβ interaction was detectable without any ERβ ligands but was enhanced by the ERα/ERβ common ligand 17-β-estradiol (E2; Figure 1A) and the ERβ-specific ligand diarylpropionitrile (DPN; Figure 1B). In contrast, the ERα-specific ligand propyl-pyrazole triol (PPT) did not have any effects on ERβ binding to EYA2 (Figure 1B).

Next, we examined the effect of EYA2 on the transcriptional activity of ERβ. MCF7 breast cancer cells express both ERα and ERβ (Supplemental Figure 1A; supplemental material available online with this article; doi:10.1172/JCI74085DS1). Therefore, both ERα-specific ligand PPT and ERβ-specific ligand DPN stimulated transcription of *pS2*, a common target gene of ERα and ERβ (Figure 1C, columns 8 and 9). In contrast, only DPN, but not PPT, activated transcription of *MDA7*, an ERβ-specific target (Figure 1C, columns 2 and 3). Ectopic expression of EYA2 repressed the transcriptional activation of *MDA7* by DPN (Figure 1C, compare columns 3 and 6), but not that of *pS2* by either DPN or PPT (Figure 1C, compare columns 7–9 with 10–12). Reciprocally, siRNA knockdown of EYA2 further enhanced the transcriptional activation of *MDA7* by DPN (Figure 1D; compare columns 3 and 6), without affecting DPN- or PPT-activated transcription of *pS2* (Figure 1D, compare columns 7–9 with 10–12). We also observed a similar repressive effect of EYA2 on ERβ-mediated transcription in MDA-MB-231 breast cancer cells, which express ERβ but not ERα (Supplemental Figure 1, A and B). Furthermore, we introduced ERα or ERβ into HEK293T cells and the breast cancer Hs578T cell line, both of which lack endogenous ERα/β expression. Again, we confirmed the ERβ-specific transcriptional repression by EYA2 on multiple ERβ-specific target genes in the ERα/β-reconstituted HEK293T (Supplemental Figure 1, C–E) and Hs578T cells (Supplemental Figure 2). Taken together, these data strongly suggest that EYA2 is a transcriptional corepressor of ERβ but not of ERα.

EYA2 inhibits ERβ transcriptional activity by directly dephosphorylating phosphorylated Y36 of ERβ. To understand how EYA2 repressed the activity of ERβ but not ERα, we first determined whether the tyrosine phosphatase activity of EYA2 was required for its transcriptional repression. We engineered 2 point mutations of EYA2 that either partially (D274A) or completely (D502A) eliminated its phosphatase activity (Supplemental Figure 3, A and B). The impaired enzymatic activity of these 2 EYA2 mutants correlated with the degree of their deficiency in repressing ERβ-mediated transcriptional activation (Supplemental Figure 3C). Furthermore, WT EYA2 significantly diminished the total tyrosine phosphorylation (p-Y) level of ERβ, whereas the 2 EYA2 mutants were deficient in reducing p-Y of ERβ (Supplemental Figure 3D). In contrast, WT EYA2 did not affect the total p-Y status of ERα (Supplemental Figure 3D). These results are consistent with the notion that EYA2 represses the transcriptional activity of ERβ by directly dephosphorylating certain phosphotyrosine residues in ERβ.

To identify the EYA2-targeted phosphotyrosine residue in ERβ, we focused on the AF1 domain of ERβ because of its sequence divergence from ERα. Indeed, an ERβ mutant lacking AF1, while still retaining partial ligand-dependent transcriptional activity, was refractory to EYA2-mediated repression (Supplemental Figure 4A). By systematically mutating individual tyrosine residues in AF1 of ERβ, we found that substitution of Y36 with either alanine (Y36A) or phenylalanine (Y36F) largely abolished the total p-Y signal of ERβ (Supplemental Figure 4, B and C). Y36 is highly conserved among ERβ orthologs in mammals, but interestingly, human and other mammalian ERα proteins have an alanine residue at the corresponding position (Figure 2A). A phosphorylated Y36–containing (p-Y36–containing) ERβ peptide was dephosphorylated efficiently by recombinant WT, but not mutant, EYA2 (Supplemental Figure 4D). This phosphopeptide was used as the antigen to raise a phospho-specific polyclonal antibody that recognized WT ERβ but not Y36F-ERβ or WT ERα (Figure 2B). The p-Y36 signal was substantially reduced by EYA2 overexpression (Figure 2C) and enhanced by EYA2 knockdown (Figure 2D), thus further validating the antibody specificity. Furthermore, we observed that p-Y36 of endogenous ERβ in MDA-MB-231 and MCF7 breast cancer cells was stimulated by ERβ agonists (Figure 2E and Supplemental Figure 4E) and dampened by EYA2 (Figure 2E). Last, recombinant WT, but not mutant EYA2, completely eliminated the p-Y36 signal of ERβ in vitro (Figure 2F). Collectively, these results unequivocally demonstrate that p-Y36 of ERβ is a direct substrate of the EYA2 tyrosine phosphatase activity.

To examine the impact of p-Y36 on ERβ-mediated transcription, we expressed WT and mutant ERβ in MDA-MB-231 breast cancer cells at levels comparable to those observed for endogenous ERβ in normal breast tissue (Supplemental Figure 4F). The Y36F mutation abolished the ligand-dependent activation of the ERβ target genes (Figure 2G, compare column 7 with 9, and 19 with 21). In contrast, a tyrosine-to-glutamate (Y36E) mutation retained the transcriptional activity of ERβ (Figure 2G, compare column 7 with 8, and 19 with 20), suggesting that a negative charge at this position was sufficient to sustain ERβ transcriptional activity. Remarkably, unlike WT ERβ, Y36E-ERβ was largely refractory to EYA2-mediated transcriptional repression (Figure 2G, compare column 10 with 11, and 22 with 23). This finding lends strong support to the notion that EYA2 represses the transcriptional activity of ERβ primarily through dephosphorylation of p-Y36. As ERα lacks a tyrosine residue at the corresponding position and its overall p-Y intensity is not affected by EYA2 (Supplemental Figure 3D), our data provide a molecular explanation for the repressive effect of EYA2 on the transcriptional activity of ERβ, not ERα.

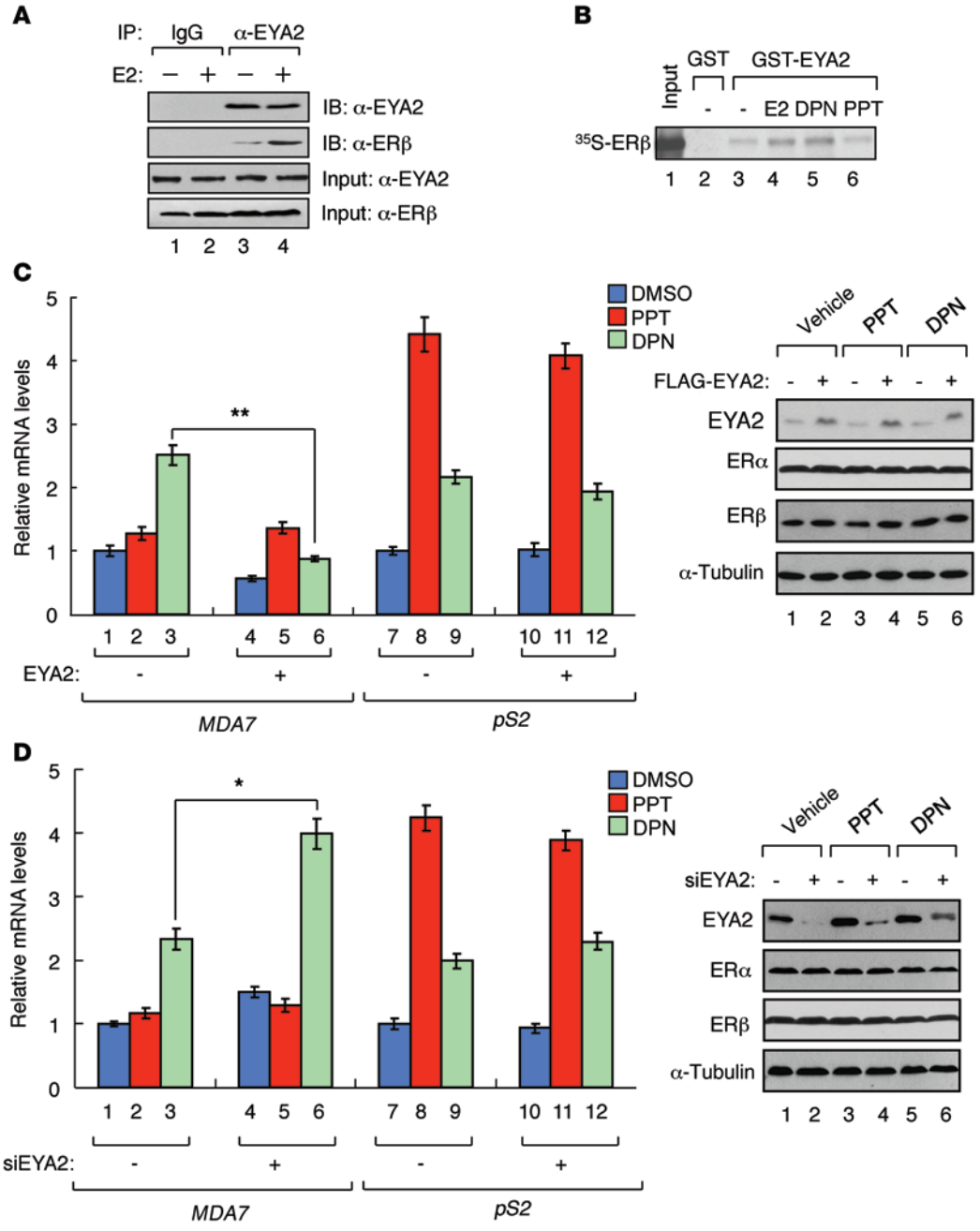

Figure 1. EYA2 modulates the transcriptional activity of ERβ but not ERα. (**A**) Co-IP of endogenous EYA2 and ERβ in a substrain of an MCF7 breast cancer cell line that expresses both ER proteins. E2 (10 nM) was used. (**B**) GST-EYA2 pulldown with in vitro–translated ERβ in the presence of vehicle or various ligands. Five percent input protein was loaded. An ERα-specific agonist, PPT (1 nM), or an ERβ-specific agonist, DPN (10 nM), was used. (**C**) Real-time RT-PCR assessed the effect of EYA2 overexpression on ERβ-mediated transcription of its target genes *MDA7* and *pS2* in MCF7 cells. The value for column 1 was set at 1. (**D**) Effects of EYA2 knockdown on ERβ-mediated transcription of *MDA7* and *pS2* in MCF7 cells. $^{*}P < 0.05$; $^{**}P < 0.01$. Gel images in this and the following figures are representatives of at least 3 independent experiments. Graphs throughout the figures represent the average of at least 3 experiments. Error bars represent SEM.

c-ABL directly phosphorylates Y36 and promotes ERβ-mediated transcriptional activation. In order to identify the tyrosine kinase that phosphorylates Y36, we screened a mammalian expression library that contains all known human tyrosine kinases. The initial screen identified c-ABL as a candidate kinase for Y36 phosphorylation. Follow-up experiments, as described below, confirmed that c-ABL directly phosphorylates Y36. First, WT c-ABL, but not a kinase-dead mutant (33), markedly increased both the total p-Y and p-Y36 levels of ERβ (Figure 3A). Second, both ectopic and endogenous c-ABL and ERβ were physically associated with each other in co-IP (Figure 3A and Supplemental Figure 5, A and B). Third, the c-ABL inhibitor imatinib reduced p-Y36 intensity (Figure 3B, compare lanes 3 and 4 with 5 and 6), whereas the c-ABL activator DPH (34) stimulated Y36 phosphorylation (Figure 3B, compare lanes 3 and 4 with 7 and 8). Fourth, knockdown of c-ABL by multiple independent siRNA oligonucleotides dampened Y36 phosphorylation (Figure 3C). Last, affinity-purified WT c-ABL protein, but not the kinase-dead mutant (35), directly phosphorylated ERβ in an in vitro kinase reaction (Figure 3D, compare lanes 3 and 4 with 6 and 7, and Supplemental Figure 5, C and D). In contrast, the Y36F mutant of ERβ was not phosphorylated by WT c-ABL (Figure 3D, lanes 9 and 10). In aggregate, these data clearly demonstrate that Y36 is the primary substrate for the c-ABL kinase activity.

To assess the functional impact of c-ABL on the transcriptional activity of ERβ, we analyzed the effect of c-ABL knockdown on ligand-stimulated transcription of the ERβ target genes. To ascertain the specificity of the siRNA knockdown, we transfected MDA-MB-231 cells with an siRNA oligonucleotide that targets the

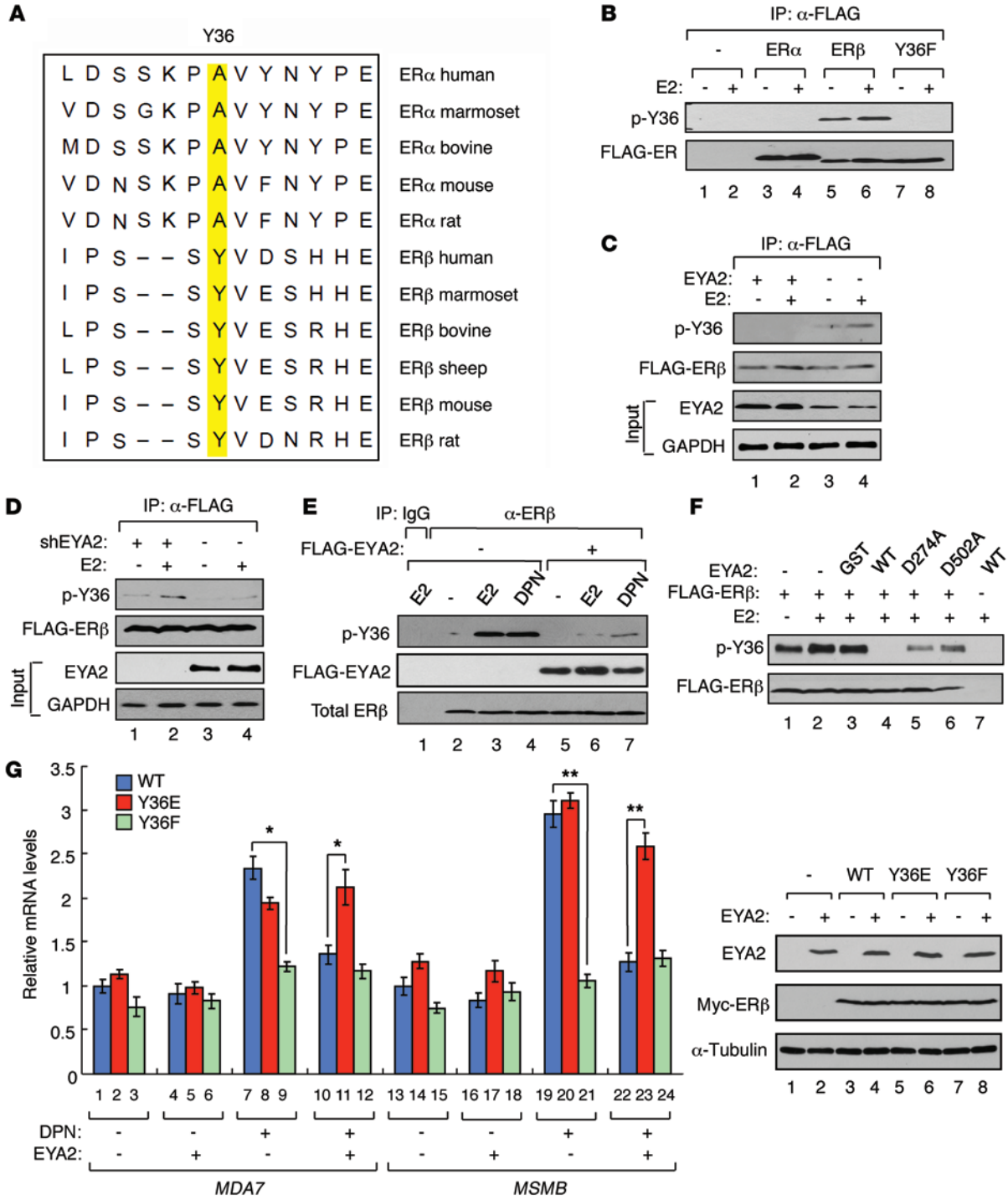

Figure 2. EYA2 inhibits ERβ transcriptional activity by directly dephosphorylating p-Y36. (**A**) Sequences of mammalian ERα and ERβ orthologs surrounding the Y36 residue of human ERβ. ClustalW was used for the sequence alignment. (**B**) The anti–p-Y36 antibody recognized WT ERβ, but not the Y36F mutant or ERα, in IP-Western blotting of FLAG-ER proteins from HEK293T cells. (**C**) IP-Western blot of FLAG-ERβ in HEK293T cells indicated that EYA2 reduced the p-Y36 signal. (**D**) EYA2 knockdown in HEK293T cells increased the p-Y36 signal of FLAG-ERβ. (**E**) Ligand-stimulated p-Y36 signal of endogenous ERβ in MDA-MB-231 cells was reduced by EYA2. EYA2-transfected cells were treated with vehicle, E2, or DPN for 2 hours. The lysates were used in an ERβ-specific IP, followed by immunoblotting with the anti–p-Y36 or anti–total ERβ antibody. (**F**) Recombinant WT EYA2, but not phosphatase-deficient mutant proteins, efficiently dephosphorylated IP FLAG-ERβ in vitro. (**G**) Real-time RT-PCR compared WT ERβ and the mutants in activation of the ERβ target genes *MDA7* and *MSMB* in MDA-MB-231 cells. Error bars represent SEM. $*P < 0.05$; $**P < 0.01$.

3′ untranslated region (3′-UTR) of the *c-ABL* gene and, for rescuing, used a WT *c-ABL* expression vector lacking the corresponding 3′-UTR sequence. c-ABL knockdown alone significantly reduced the DPN-stimulated mRNA levels of *MDA7* and *MSMB*, 2 ERβ target genes (Figure 3E, compare lane 4 with 5, and 10 with 11). Cotransfection of the siRNA-resistant cDNA clone of *c-ABL* rescued the knockdown effect (Figure 3E, lanes 6 and 12), thus validating the role of c-ABL in supporting ERβ-dependent transcription.

To determine whether the c-ABL effect on ERβ-dependent transcription was through phosphorylation of Y36, we compared the effect of c-ABL knockdown on WT ERβ, Y36F, and Y36E mutants. While Y36F remained transcriptionally inactive upon c-ABL knockdown (Figure 3F, compare lane 9 with 12, and 21 with 24), the transcriptionally active yet nonphosphorylatable Y36E mutant was refractory to c-ABL knockdown (Figure 3F, compare lane 8 with 11, and 20 with 23). This is reminiscent of the observed recalcitrance of the same ERβ mutant to the transcriptional repression by EYA2 (Figure 2G). Taken together, these enzymatic and transcriptional results firmly establish a functional relationship between c-ABL and EYA2 and their common downstream target, Y36 of ERβ.

p-Y36 promotes the interaction between ERβ and its coactivator. To elucidate the molecular basis for the role of p-Y36 in transcriptional activation, we first compared the ability of WT ERβ and Y36 mutants to bind to p300, one of the known transcriptional coactivators of ERβ (36, 37). The Y36F mutant had a significantly reduced affinity for p300 as compared with WT ERβ (Figure 4A, compare lanes 3 and 4 with 5 and 6). In contrast, the Y36E mutant had a somewhat higher affinity for p300 than did WT ERβ (Figure 4A, lanes 7 and 8; also see quantification).

We next used chromatin immunoprecipitation (ChIP) to compare the ability of WT ERβ and the Y36F mutant to recruit p300 to the ERβ target promoters. Consistent with published studies of ERα (38), E2 treatment stimulated cyclic recruitment of p300 to the ERβ target promoters in WT ERβ–expressing cells (blue lines in Figure 4, B and C). In contrast, cells expressing the Y36F mutant exhibited substantially attenuated ligand-dependent recruitment of p300 (red lines in Figure 4, B and C). This was not due to reduced chromatin binding of the Y36F mutant to these promoters (Figure 4, D and E). In fact, more Y36F was associated with the promoter regions than was WT ERβ. In a separate ChIP, we found that EYA2 also reduced promoter recruitment of p300 (Figure 4, F and G, and Supplemental Figure 2C), which phenocopied the mutational effect of Y36F (Figure 4, B and C). These data strongly indicate that p-Y36 is important for ERβ-mediated coactivator binding and promoter recruitment.

The p-Y36 signaling circuitry regulates the antitumor activity of ERβ. To determine the importance of the p-Y36 signaling circuitry in the antitumor function of ERβ, we first compared the effects of WT and mutant ERβ proteins on tumor cell growth. Consistent with published work (3–6), WT ERβ significantly reduced the growth of breast cancer cells in both tissue culture (Supplemental Figure 6, A and B) and xenograft models (Figure 5, A and B, and Supplemental Figure 7, A and B). In contrast, the transcriptionally inactivating Y36F mutation completely abolished ERβ antitumor activity (Figure 5A and Supplemental Figure 6A). On the other hand, the transcriptionally active Y36E mutant inhibited tumor cell growth as robustly as did the WT protein (Figure 5B and Supplemental Figure 6B). These results clearly indicate that p-Y36 is important for the antitumor activity of ERβ.

Next, we sought to validate the relevance of EYA2 and c-ABL to the antitumor activity of ERβ. Consistent with the previous reports of the oncogenic activity of EYA2 (22, 23) in breast cancer, ectopic expression of EYA2 promoted breast cancer cell growth in vitro and in vivo (Supplemental Figure 6, C and D). Using the same systems, we found that knockdown of c-ABL led to accelerated tumor cell growth (Supplemental Figure 6, E and F). We reasoned that if the effects of EYA2 and c-ABL on tumor cell growth were mediated by the phosphorylation status of Y36-ERβ, they would differentially influence the antitumor activity of WT ERβ and the functionally active yet nonphosphorylatable Y36E mutant. Indeed, both in vitro and in vivo studies showed that EYA2 substantially neutralized the antitumor activity of WT ERβ, but not that of the Y36E mutant (Figure 5C, Supplemental Figure 7C, and Supplemental Figure 8, A and B). Likewise, the same Y36E mutant was relatively refractory to c-ABL knockdown as compared with WT ERβ (Figure 5D, Supplemental Figure 7D, and Supplemental Figure 8, C and D). Therefore, Y36E-ERβ retains the antitumor activity of WT ERβ but circumvents the control by c-ABL and EYA2. Based on these findings, we conclude that EYA2 and c-ABL regulate the antitumor activity of ERβ predominantly via their influence over the phosphorylation status of the Y36 residue.

High p-Y36 levels are a prognostic marker for breast cancer progression and predict longer survival. To explore the clinical significance of this newly discovered signaling circuitry, we conducted immunohistochemistry (IHC) of breast cancer tissue samples. First, the specificity of the antibodies for p-Y36, EYA2, and c-ABL used in the IHC analysis was verified by antigen competition (Supplemental Figure 9, A–C). In particular, prominent nuclear staining of breast tumor cells with the p-Y36 antibody was abolished by preincubation of the antibody with a p-Y36–containing peptide, but not its nonphosphorylated counterpart (Supplemental Figure 9C). In addition, siRNA knockdown of endogenous ERβ in MDA-MB-231 cells abolished the p-Y36 signal in both IP-Western blotting and IHC (Supplemental Figure 9, D and E), thus further corroborating the specificity of this antibody.

Using a cohort of 104 human breast tumor samples in our initial study, we found a markedly positive correlation ($P=7.46\times10^{-6}$) between c-ABL and p-Y36 levels and a negative correlation ($P = 2.89 \times 10^{-5}$) between EYA2 and p-Y36 levels (Figure 6A and Supplemental Table 1). This is consistent with the opposite effects of c-ABL and EYA2 on the p-Y36 status and ERβ functions observed in our preclinical studies. Using the available survival information of 56 subjects from this cohort, we observed a strong correlation between positive p-Y36 staining and longer disease-free ($P = 0.001$) and overall survival ($P = 0.005$; Supplemental Figure 10A).

To validate the clinical correlation, we used a prognostic tissue microarray (TMA) from the National Cancer Institute (NCI), which consists of a larger cohort of breast tumor samples with a clinical follow-up record. Using a total of 726 readable IHC samples, we found that the p-Y36 signal was inversely correlated with tumor size ($P = 1.1 \times 10^{-6}$), positive node status ($P = 0.034$), advanced disease stage ($P = 8.86 \times 10^{-6}$), and increased tumor grade ($P = 0.007$), thus demonstrating a significant correlation between loss of p-Y36

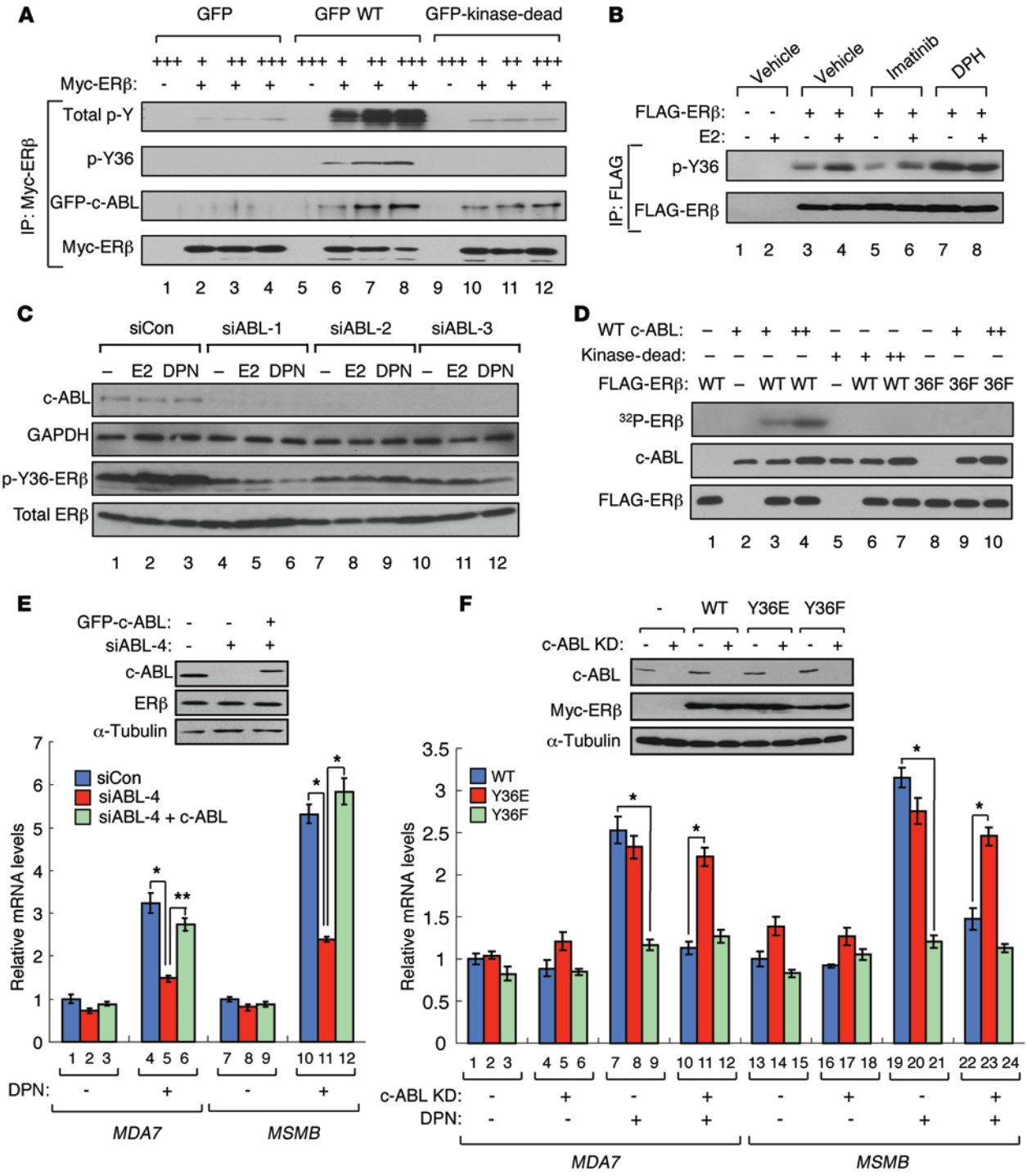

Figure 3. c-ABL directly phosphorylates Y36 and promotes ERβ-mediated transcriptional activation. (**A**) WT c-ABL, not a kinase-dead mutant, increased total p-Y and p-Y36–specific signals of FLAG-ERβ in HEK293T cells. Immunoblotting with an anti–c-ABL antibody indicated the physical association between c-ABL and ERβ. (**B**) p-Y36 of FLAG-ERβ was reduced by imatinib but enhanced by DPH, a c-ABL activator, in HEK293T cells. (**C**) c-ABL knockdown reduced p-Y36 of endogenous ERβ in MDA-MB-231 cells. (**D**) WT ERβ was directly phosphorylated in vitro by purified WT, but not mutant, c-ABL. (**E**) c-ABL knockdown reduced transcription of the ERβ target genes *MDA7* and *MSMB* in MDA-MB-231 cells, which was rescued by an siRNA-resistant c-ABL expression vector. (**F**) c-ABL knockdown in MDA-MB-231 cells abolished transcriptional activation of *MDA7* and *MSMB* by WT ERβ but not the nonphosphorylatable Y36E mutant. Also included is the Y36F mutant. Error bars represent SEM. $^*P < 0.05$.

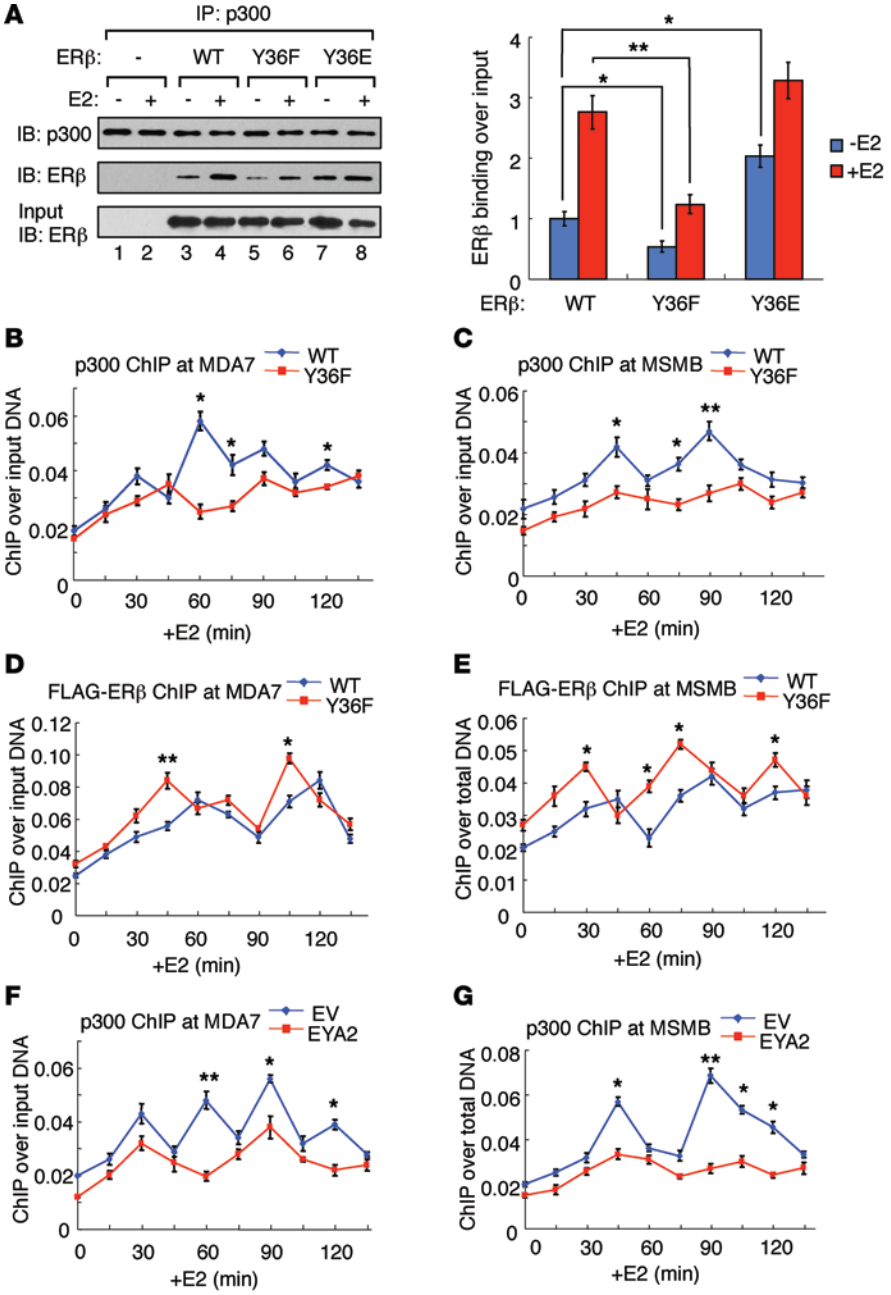

Figure 4. p-Y36 promotes interaction between ERβ and its coactivator. (**A**) Co-IP in HEK293T cells between FLAG-ERβ proteins and endogenous p300. Shown on the right is normalized quantification of the immunoblots from 3 independent experiments. (**B** and **C**) p300 ChIP at the p-Y36–dependent ERβ target promoters *MDA7* (**B**) and *MSMB* (**C**), using chromatin from Hs578T cells that expresses either FLAG-tagged WT or mutant Y36F-ERβ. In all ChIP experiments, E2 (10 nM) was added to the estrogen-deprived cells. (**D** and **E**) FLAG-ERβ ChIP at the MDA7 (**D**) and MSMB (**E**) promoters. (**F** and **G**) p300 ChIP at the same ERβ target promoters, with or without EYA2 overexpression. Error bars represent SEM. $^{*}P < 0.05$; $^{**}P < 0.01$. EV, empty vector.

and disease progression (Supplemental Figure 10B and Supplemental Table 1). Patients with p-Y36–negative tumors had shorter disease-free ($P = 0.006$) and overall ($P = 0.013$) survival than those with p-Y36–positive tumors (Figure 6B, left graphs). Most strikingly, the association with survival was only seen in stage II and III disease, consistent with an effect of p-Y36 on disease progression (Figure 6B, right graphs, and Supplemental Figure 10C). As a comparison, we also performed IHC of total ERβ using a previously validated commercial antibody (ref. 39 and Supplemental Figure 11A). None of the ERβ-negative samples stained positive for p-Y36 (data not shown), further corroborating the specificity of p-Y36. Unlike p-Y36, we did not find a statistically significant correlation between total ERβ and disease progression when all disease stages were combined (Figure 6C, left graphs). When only stage II and III cases were considered, total ERβ levels correlated with overall ($P = 0.002$), but not disease-free ($P = 0.134$), survival (Figure 6C, right graphs, and Supplemental Figure 11B). For stage II and III breast cancer patients, we performed univariate and multivariate analyses to determine the relationship between disease-free survival and overall survival and tumor size, nodal status, grade, and ERα, PR, HER2, ERβ, and p-Y36 status (Supplemental Table 2). In multivariate analysis, p-Y36 status (but not total ERβ), tumor size, and nodal status remained independent predictors of overall survival, whereas tumor size, nodal status, grade, and ERα status were independent predictors of disease-free survival. Collectively, these findings of disease correlation underscore the clinical relevance of the previously unappreciated p-Y36–centered signaling circuitry.

Discussion

Our work identifies an ERβ-specific phosphotyrosine residue that serves as a molecular switch for the transcriptional and antitumor activities of ERβ. In the model shown in Figure 7, we propose that c-ABL and EYA2 form a signaling circuitry together with p-Y36 of ERβ. As a consequence of the antagonistic actions of c-ABL and EYA2, p-Y36 status dictates the functional interaction between ERβ and its coactivators. This in turn leads to transcriptional activation of ERβ-specific target genes and inhibition of tumor cell growth. This model is based on compelling data from our mechanistic work in vitro and is further bolstered by strong in vivo evidence from the tumor growth study. In particular, the fact that the Y36E mutant retained ERβ function but bypassed control by c-ABL and EYA2 unequivocally establishes p-Y36 as the functional "lynchpin" linking ERβ with its upstream regulators. Importantly, there was a stronger association of p-Y36-ERβ positivity with a good clinical outcome compared with total ERβ, further indicating the clinical relevance of this specific p-Y36–centered signaling circuitry and its potential as a therapeutic target.

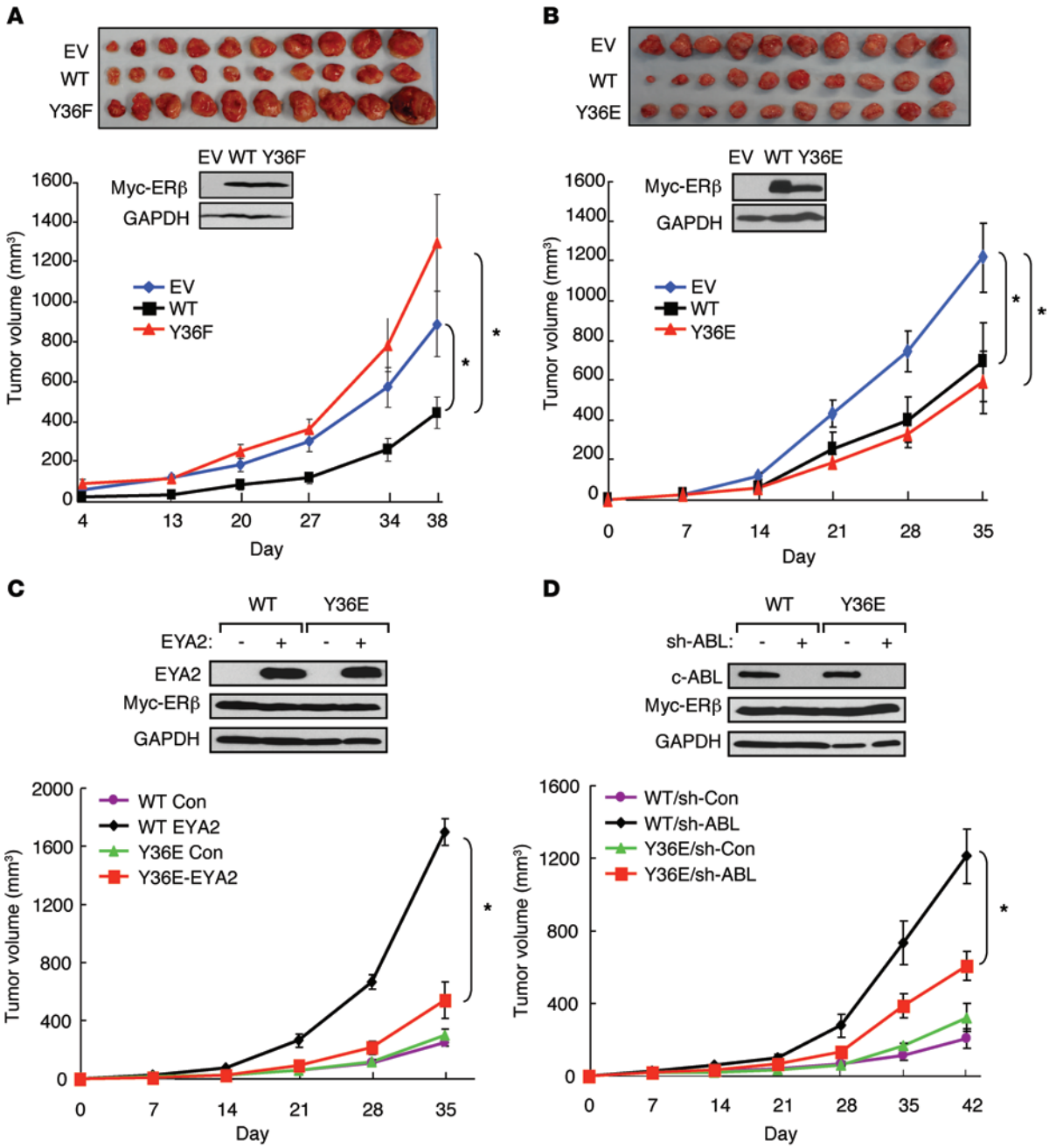

Figure 5. p-Y36 is important for the antitumor activity of ERβ. (**A** and **B**) Xenograft tumor growth derived from MDA-MB-231 cells that contained empty vector, WT, or mutant ERβ. The Myc-ERβ proteins and images of individual tumors upon harvest are shown. (**C**) EYA2 overexpression in MDA-MB-231 cells neutralized the antitumor activity of WT, but not Y36E-mutant, ERβ. (**D**) Y36E mutant was more resistant to c-ABL knockdown than was WT ERβ in the xenograft tumor model. Error bars represent SEM. *$P < 0.05$.

The opposing actions of EYA2 and c-ABL on the p-Y36 status of ERβ can at least partly account for their reported activities in breast cancer. EYA2 has been shown to promote growth and invasion of breast cancer cells (22), whereas c-ABL is reported to have a tumor-suppressive activity, at least under certain contexts (29, 30). However, c-ABL knockdown still increased tumor cell growth to some extent, even in the presence of the constitutively active ERβ mutant, suggesting that c-ABL most likely has additional functionally important targets besides ERβ in breast cancer cells. These findings are consistent with a complex and multifaceted role of c-ABL in solid tumors (26, 40). Likewise, EYA2 may also have other substrates in addition to ERβ in promoting breast cancer progression. Nevertheless, our data clearly indicate that both c-ABL and EYA2 exert their opposing actions on the antitumor activity of ERβ primarily through Y36.

Previous work has also implicated certain phosphoserine residues of ERβ in the regulation of ERβ transcriptional activity (41–45). It will be of interest to determine whether p-Y36 and the previously identified modification events can act cooperatively or antagonistically to regulate ERβ activity in the transcription and

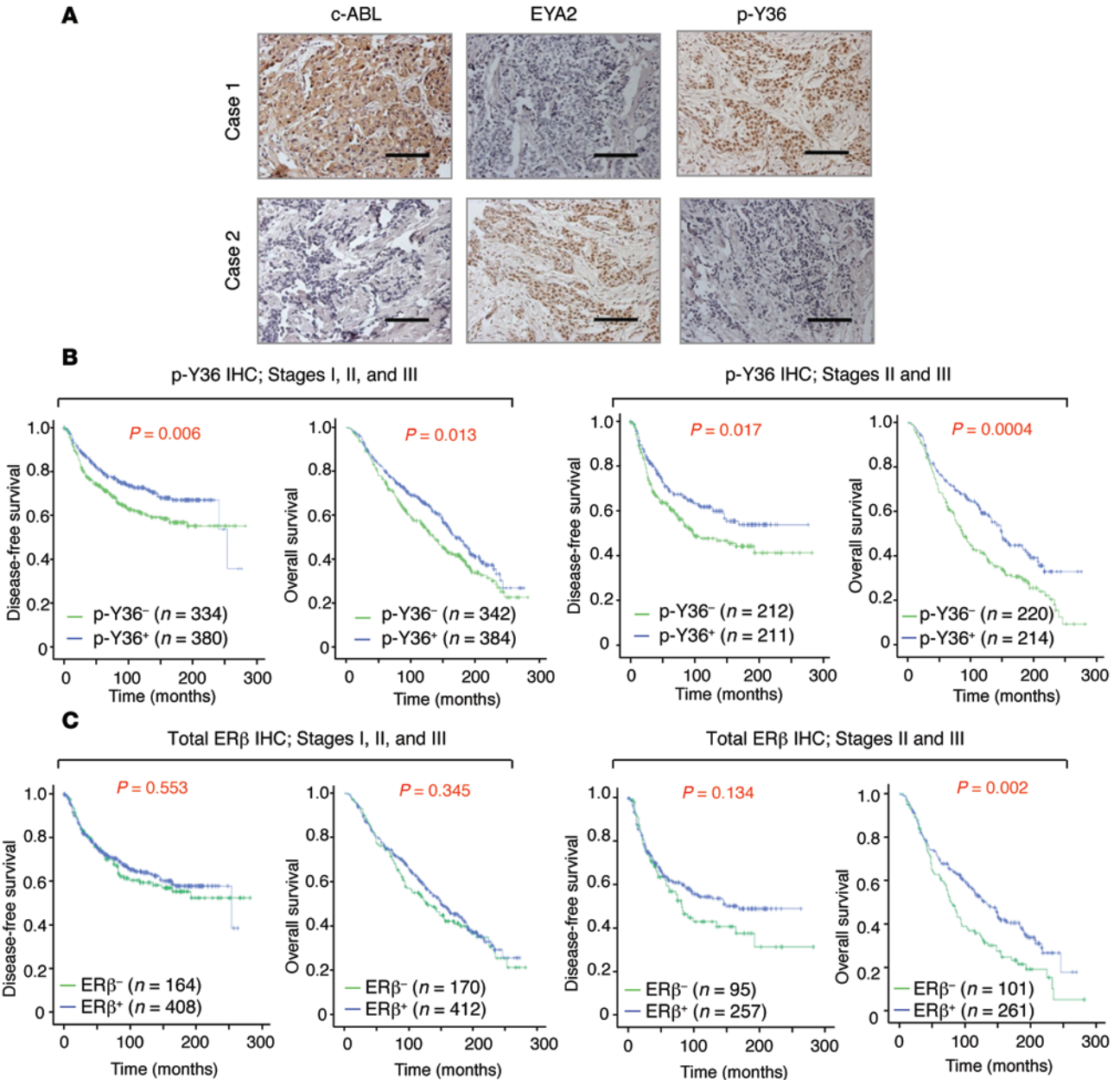

Figure 6. Clinical correlation of p-Y36 in breast cancer. (**A**) Expression of p-Y36, c-ABL, and EYA2 in human breast cancer tissues. Left panels: Representative IHC staining of p-Y36, c-ABL, and EYA2. Original magnification, ×20; scale bars: 100 μm. (**B**) Kaplan-Meier estimate of disease-free survival and overall survival in a total of 726 available specimens from the TMA (left graphs) and the stage II and III specimens from the TMA (right graphs), stained with the p-Y36 antibody. Marks on the graph lines represent censored samples. (**C**) Kaplan-Meier estimate of disease-free survival and overall survival in the total (left graphs) and the stage II and III specimens (right graphs) stained for total ERβ.

inhibition of tumor growth. While glutamate (E) is generally considered an effective phosphomimetic substitution for serine or threonine, E is structurally distinct from Y. Thus in many cases, the Y-to-E mutation has the same effect on protein function as Y-to-A or Y-to-F mutations. In this regard, it is somewhat surprising that the Y36E mutant of ERβ fully retained its transcriptional and antitumor activities. This unusual property of the Y36E mutant allowed us to definitively validate the specific functional relationship between p-Y36 and its upstream regulators c-ABL and EYA2. Given the size difference between p-Y and E, it is unlikely that p-Y36 is directly involved in ERβ interaction with its coactivators. Rather, the negative charge at this position likely induces a conformational change in ERβ that in turn facilitates coactivator binding to other parts of ERβ.

Historically, the antitumor activity of ERβ has not been extensively exploited for breast cancer treatment. In addition, uncertainty over the clinical significance of the abundance of total ERβ further complicates efforts to develop ERβ-related agents for clinical use. Our study of 2 independent clinical cohorts clearly indicates a significant correlation between tumor p-Y36 status and patient survival, which substantially strengthens the clinical relevance of our mechanism-based findings. Notably, p-Y36 status correlated

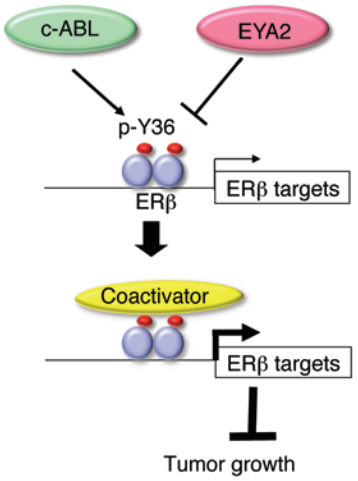

Figure 7. A model for the p-Y36–centered signaling circuitry.

with survival in stage II and III disease, whereas no correlation was seen in stage I disease, consistent with the predicted effect of p-Y36 on disease progression. In support of the functional importance of p-Y36 for the antitumor activity of ERβ, we found that its intensity was a more robust prognostic marker than total ERβ. It will be of importance to further evaluate the clinical utility of p-Y36 in predicting disease outcome and/or therapeutic response.

Given the druggable nature of all 3 components in the newly discovered signaling pathway (ERβ/EYA2/c-ABL), our findings may inform the development of new approaches for breast cancer therapies. Of note, approximately half of the triple-negative breast cancer cases express ERβ (11), making stimulation of ERβ antitumor activity an attractive therapeutic possibility for this aggressive subtype of breast cancer that currently lacks any target therapies. Indeed, there has been increasing interest in treating breast cancer and other ERβ-expressing cancers with ERβ-specific agonists (10). The safety and drug tolerance of at least 1 ERβ agonist, S-equol, have been demonstrated by 2 completed and published clinical trials (46, 47). Furthermore, small-molecule EYA2 inhibitors and c-ABL activators are available for preclinical studies (34, 48). Given the oncogenic property of EYA2 and the context-dependent antitumor activity of c-ABL in the breast cancer literature (21–23, 29, 30), it is conceivable that ERβ agonists synergize with c-ABL activators and/or EYA2 inhibitors in inhibiting those breast tumors in which the p-Y36–centered signaling circuitry is functional.

Methods

Plasmids. The expression vectors for ERα and ERβ (49) and GFP-fused c-ABL constructs (33) were described previously. ERβ AF1 and AF2 deletion constructs were made by standard PCR. The FLAG- and Myc-tagged EYA2 were constructed using pcDNA3 (Invitrogen) and the pCDH-EF1-MCS-T2A-Puro lentiviral expression vector (System Biosciences), respectively. The shRNA targeting sequence for EYA2, CATACCAACCTACTGCAGA, was inserted into the pSilencer 2.1-U6 neo vector (Ambion). Plasmids encoding GST fusion proteins were constructed in pGEX-KG (Amersham Biosciences, GE Healthcare). EYA2 (D274A), EYA2 (D502A) and ERβ Y36 mutations were generated by the QuikChange site-directed mutagenesis kit (Stratagene). The WT and kinase-dead mutant GFP-c-ABL constructs were provided by Robert Clark (University of Texas Health Science Center at San Antonio).

Cell lines and reagents. Parental cell lines were purchased from ATCC and cultured per the manufacturer's instructions. Hs578T derivatives containing the doxycycline-inducible FLAG-ER expression system were provided by John R. Hawse and Thomas C. Spelsberg (Mayo Clinic, Rochester, Minnesota, USA) (50). The Hs578T derivatives were cultured in phenol red-free DMEM medium with 10% FBS, supplemented with 5 mg/l blasticidin S (Invitrogen) and 500 μg/ml zeocin (Invitrogen). To establish stable cell pools with ectopic expression of EYA2 or ERβ, the corresponding lentiviruses were prepared in HEK293T cells and were used to infect various breast cancer cell lines. Stable cell pools or clones were established by selection in 2 μg/ml puromycin (Invitrogen). The HEK293 cells with inducible expression of WT and kinase-dead mutant c-ABL were previously described (35). E2, PPT, and DPN were obtained from Tocris Bioscience. Imatinib mesylate and DPH were purchased from Selleck Chemicals (S1026) and Sigma-Aldrich (SML0202), respectively.

Antibodies. The following commercially available antibodies were used: anti-FLAG M2 (A8592 and F3165; Sigma-Aldrich), anti-ERα (HC20, sc-543; Santa Cruz Biotechnology Inc.), anti-ERβ for immunoblotting (14C8; GeneTex; 9.88; Abcam), anti-ERβ for IP (EPR3777; Novus), anti-ERβ for IHC (68-4; Millipore), anti-EYA2 (HPA027024; Sigma-Aldrich), anti-pTyr (PY99, sc-7020; Santa Cruz Biotechnology Inc.), anti-p300 (sc-584; Santa Cruz Biotechnology Inc.), anti-GAPDH (G9295; Sigma-Aldrich), anti–FLAG-HRP (A8592; Sigma-Aldrich), anti–c-ABL (24-11, sc-23; Santa Cruz Biotechnology Inc.), and anti–FLAG M2 agarose (A2220; Sigma-Aldrich). Two anti–p-Y36 antibodies were raised against the ERβ p-Y36–containing peptide SIYIPSS(pY)VDSHHE: 1 in chicken (GenWay Biotech Inc.) and 1 in rabbit (Epitomics, Abcam). Both were used interchangeably in Western blot analysis, and the rabbit antibody was used in IHC.

Yeast 2-hybrid screen. The bait plasmid pGBKT7-ERβ (1-148) and a human mammary cDNA prey library (Clontech) were sequentially transformed into *Saccharomyces cerevisiae* strain AH109 according to the manufacturer's protocol. Transformants were grown on a synthetic medium lacking tryptophan, leucine, adenine, and histidine, but containing 1 mM 3-aminotriazole.

Co-IP and GST pulldown assays. Co-IP was performed as previously described (51). For the GST pulldown assay, GST fusion proteins were expressed and purified according to the manufacturers' instructions (Amersham Pharmacia and QIAGEN). ^{35}S-labeled, in vitro–translated proteins were incubated with the GST fusion proteins bound to GST beads (Amersham Biosciences), and the pulldown proteins were analyzed as previously described (51).

Transient transfection. All cells assessed for ligand stimulation were cultured in phenol red-free medium containing 5% charcoal stripped (CS) FBS for 3 days, reseeded in 24-well Nunclon plates (Fisher Scientific), and transfected with various vectors as indicated in the individual figures (Figure 2, B–D, Figure 3, A–C, Figure 4A, and Supplemental Figure 4A) using Lipofectamine 2000 (Invitrogen) according to the manufacturer's instructions. Six hours after transfection, cells were treated for 24 hours with either vehicle or ligand at the indicated final concentration. For screening a human tyrosine kinase library (Addgene), individual kinase expression vectors were cotransfected with a Myc-tagged ERβ expression vector into HEK293T cells.

For the luciferase assay, *Renilla* luciferase reporter vector phRL-SV40 (Promega) was used as an internal control. Luciferase values were normalized as described previously (52).

Real-time RT-PCR. RNA was extracted with TRIzol reagent (Invitrogen). cDNA was synthesized with 1 μg of total RNA using the ImPromII Reverse Transcription System (Promega) and random primers. Quantitative PCR (qPCR) was conducted using the 7900HT Real-Time PCR System (Applied Biosystems). The level of *GAPDH* mRNA was measured as the internal control.

ChIP. For ChIP experiments in the ERβ-inducible Hs578T cells, 100 ng/ml doxycycline was added for 24 hours. Before harvesting, cells were treated with either ethanol (vehicle) or 10 nM E2 for various times. Cells were crosslinked with 1% formaldehyde for 10 minutes, treated with glycine at a final concentration of 0.125 M for 5 minutes at room temperature, and lysed in lysis buffer (5 mM HEPES, pH 9.0, 85 mM KCl, 0.5% Triton X-100) for 15 minutes on ice. Nuclei were resuspended in nuclei lysis buffer (50 mM Tris-HCl, pH 8.0, 10 mM EDTA, 1% SDS), and the crosslinked DNA was sonicated for 10 minutes (with a 30-second on/off cycle) using a Bioruptor sonicator (Diagenode). The supernatant was used for ChIP as previously described (53).

In vitro tyrosine kinase assay. The tyrosine kinase assay was performed as described previously (54). Briefly, FLAG-ERβ was affinity purified from transiently transfected HEK293T cells. WT and kinase-dead mutant FLAG-c-ABL proteins were inducibly expressed in HEK293 cells (35) and purified in a similar fashion. ERβ and c-ABL proteins were then incubated in kinase buffer (50 mM HEPES, 10 mM $MgCl_2$, 1 mM DTT, 2.5 mM EGTA, 0.1 mM Na_3VO_3, 1 mM NaF) containing γ-^{32}P-ATP at 30°C for 30 minutes. Kinase reactions were resolved by SDS-PAGE and exposed by autoradiography.

In vitro tyrosine phosphatase assay. Commercially synthesized phosphopeptides or FLAG-ERβ proteins IP from HEK293T cells were used as the substrates. The peptide sequences are as follows: p-Y142-H2AX(20): CPSGGKKATQASQE(pY); p-Y36-ERβ: SIYIPSS(pY)VDSHHE. WT and mutant GST-EYA2 proteins were incubated with substrates in phosphatase buffer (50 mM Tris-HCl, pH 7.0, 5 mM $MgCl_2$, 10% glycerol, 3 mg/ml BSA) at 37°C for 30 minutes. Release of free phosphate was detected using the Malachite Green detection assay according to the manufacturer's instructions (BIOMOL, Enzo Life Sciences) (19).

Xenograft assay. Forty-five-day-old female athymic nude mice (Harlan) were injected orthotopically with MDA-MB-231 cells into mammary gland fat pads. Tumor development was followed by caliper measurements along 2 orthogonal axes: length (L) and width (W). The volume (V) of tumors was estimated by the formula $V = L \times (W^2)/2$.

Human tissue analysis. Rabbit anti-EYA2 (HPA027024; Sigma-Aldrich), anti–c-ABL (sc-887; Santa Cruz Biotechnology Inc.), anti–total ERβ (68-4; Millipore), and anti–p-Y36 antibodies were used as the primary antibodies for IHC. For the larger cohort study, we purchased the Breast Cancer TMAs from the NCI Cancer Diagnosis Program. The TMAs contained 1,169 nonmetastatic breast tissue specimens divided into TNM stages I–III. IHC of formalin-fixed, paraffin-embedded samples was performed as described previously (49). After staining, a total of 726 and 582 specimens from TMAs (age range, 25 to 96 years; mean ± SD, 59.1 ± 13.4; median, 60 years) were available for analysis of p-Y36 and total ERβ, respectively. The other samples were either inadvertently detached from the case set during IHC or contained too few cells.

Each specimen was assigned a score according to the intensity of the nucleic and/or cytoplasmic staining (no staining = 0; weak staining = 1; moderate staining = 2; strong staining = 3) and the extent of stained cells (0% = 0; 1%–24% = 1; 25%–49% = 2; 50%–74% = 3; 75%–100% = 4). The final immunoreactive score was determined by multiplying the intensity score with the score of the extent of stained cells, ranging from 0 (the minimum score) to 12 (the maximum score). We defined a score of 0 as total ERβ negative, p-Y36 negative, and EYA2 negative; a score greater than 1 as total ERβ positive, p-Y36 positive, and EYA2 positive; and a score between 0 and 6 as c-ABL negative and greater than 6 as c-ABL positive.

Oligonucleotides. The following c-ABL siRNA oligonucleotides were used: siABL-1 (GACAUCACCAUGAAGCACA); siABL-2 (CUCCAUUGCUCCCUCGAAA); siABL-3 (GCAACAAGCCCACUGUCUA); and siABL-4 (CCAGCUCUACUACCUACGU). The primers for RT-PCR and ChIP assays were designed by the Affymetrix Primer Express software program. The following primers were used for mRNA analysis: MDA7-qF (CTTTGTTCTCATCGTGTCACAAC); MDA7-qR (TCCAACTGTTTGAATGCTCTCC); MSMB-qF (CCAGGAGATTCAACCAGGAA); MSMB-qR (GAAACAAGGGTGCAACATGA); NKG2E-qF (GCCAGCATTTTACCTTCCTCAT); NKG2E-qR (AACATGATGAAACCCCGTCTAA); HAVCR2-qF (GAAGAAGAAGCAGTGACGGG); HAVCR2-qR (TGTCAGAATTGTGCTAGGCG); PLA2G4D-qF (AGCCCCGGATCTGCTTTCT); PLA2G4D-qR (GGTGAGGTCATACCAGGCATC); pS2-qF (CCCCGTGAAAGACAGAATTGT); pS2-qR (GGTGTCGTCGAAACAGCAG); GREB1-qF (CAAAGAATAACCTGTTGGCCCTGC); and GREB1-qR (GACATGCCTGCCCTCTCATACTTA). The primers used for ChIP analysis were: MDA7-F3 (CCCCATCGCTGTATTGTCCT); MDA7-R3 (GGAAAAAGAGGGAGGTGGAGA); MSMB-F1 (GTCACTGGAAGGCACACAGA); MSMB-R1 (CTTGTGCCAAGAAAGCCTGT); NKG2E-F1 (AGCCACCCAAAGTCTCCTAT); NKG2E-R1 (TTCAGTGGAGAGGTCAGGTT); HAVCR2-F1 (CACTCTGCAATGCTATGGGA); HAVCR2-R1 (AGCTCACAGGCTGAGTGGTT); PLA2G4D-F1 (CTACTGGACAGTGCTGTT); and PLA2G4D-R1 (ATGGATGGGAATTAGGATACTT).

Statistics. Statistical significance in the preclinical experiments was assessed by a 2-tailed Student's *t* test. The correlation between p-Y36 expression and clinicopathologic characteristics was determined using Pearson's χ^2 test. Disease-free survival was defined as the time from the date of diagnosis to first recurrence (local or distant) or death from breast cancer without a recorded relapse. Overall survival was defined as the time from the date of diagnosis to death, in which breast cancer was the primary or underlying cause of death. Patients who were alive at the last follow-up were censored on the last follow-up date, and patients who died from causes other than breast cancer were censored at the time of death. Estimation of disease-free survival and overall survival was performed using the Kaplan-Meier method, and differences between survival curves were determined with the log-rank test. A Cox regression model was applied to determine whether a factor was an independent predictor of survival in multivariate analysis. All statistical tests were 2 sided. Statistical calculations were performed using SPSS 13.0. In all assays, $P < 0.05$ was considered statistically significant.

Study approval. For analysis of a correlation between p-Y36 and EYA2 or c-ABL, deidentified breast cancer samples were obtained with the informed consent of patients, following protocols approved by the

IRB of the Beijing Institute of Biotechnology and the Affiliated Hospital of Chinese Academy of Military Medical Sciences. All procedures involving animals and their care were approved by and conducted in conformity with the guidelines of the IACUC of the University of Texas Health Science Center at San Antonio.

Acknowledgments

We thank John R. Hawse and Thomas C. Spelsberg for the ER-inducible Hs578T breast cancer cell lines, Robert Clark for the GFP-c-ABL constructs, Rohit Jadhav for bioinformatics analysis, and Ratna Vadlamudi and Subrata Haldar for critical reading of the manuscript. The work was supported by grants from the China Major State Basic Research Development Program (2011CB504202 and 2012CB945100, to Q. Ye); the National Natural Science Foundation (81330053 and 81272913, to Q. Ye); the Cancer Prevention Research Institute of Texas (RP110524, to R. Li); the Institute for Integration of Medicine and Science (IIMS, to R. Li); the Cancer Therapy and Research Center of the University of Texas Health Science Center at San Antonio (P30CA054174, to R. Li); the NCI (CA170306, to Y. Hu, CA164122, to T.J. Curiel, and CA161349, to R. Li); the Lupus Research Institute; and the Holly Beach Public Library (to T.J. Curiel).

Address correspondence to: Rong Li, Department of Molecular Medicine, Institute of Biotechnology, University of Texas Health Science Center at San Antonio, 7703 Floyd Curl Drive, San Antonio, Texas 78229, USA. Phone: 210.562.4152; E-mail: lir3@uthscsa.edu. Or to: Qinong Ye, Department of Medical Molecular Biology, Beijing Institute of Biotechnology, 27 Tai-Ping Lu Rd., Beijing 100850, China. Phone: 8610.6818.0809; E-mail: yeqn66@yahoo.com.
Zhi-Min Yuan's present address is: Department of Genetics and Complex Diseases, Harvard School of Public Health, Boston, Massachusetts, USA.

1. Thomas C, Gustafsson JA. The different roles of ER subtypes in cancer biology and therapy. *Nat Rev Cancer*. 2011;11(8):597–608.
2. Deroo BJ, Buensuceso AV. Minireview: estrogen receptor-β: mechanistic insights from recent studies. *Mol Endocrinol*. 2010;24(9):1703–1714.
3. Hartman J, Lindberg K, Morani A, Inzunza J, Strom A, Gustafsson JA. Estrogen receptor β inhibits angiogenesis and growth of T47D breast cancer xenografts. *Cancer Res*. 2006;66(23):11207–11213.
4. Mak P, Leung YK, Tang WY, Harwood C, Ho SM. Apigenin suppresses cancer cell growth through ERβ. *Neoplasia*. 2006;8(11):896–904.
5. Hodges-Gallagher L, Valentine CD, El Bader S, Kushner PJ. Estrogen receptor β increases the efficacy of antiestrogens by effects on apoptosis and cell cycling in breast cancer cells. *Breast Cancer Res Treat*. 2008;109(2):241–250.
6. Thomas C, et al. ERβ1 represses basal breast cancer epithelial to mesenchymal transition by destabilizing EGFR. *Breast Cancer Res*. 2012;14(6):R148.
7. Nanni S, et al. Endothelial NOS, estrogen receptor β, and HIFs cooperate in the activation of a prognostic transcriptional pattern in aggressive human prostate cancer. *J Clin Invest*. 2009;119(5):1093–1108.
8. Mak P, et al. ERbeta impedes prostate cancer EMT by destabilizing HIF-1α and inhibiting VEGF-mediated snail nuclear localization: implications for Gleason grading. *Cancer Cell*. 2010;17(4):319–332.
9. Nakajima Y, et al. Estrogen regulates tumor growth through a nonclassical pathway that includes the transcription factors ERβ and KLF5. *Sci Signal*. 2011;4(168):ra22.
10. Gallo D, De Stefano I, Grazia Prisco M, Scambia G, Ferrandina G. Estrogen receptor β in cancer: an attractive target for therapy. *Curr Pharm Des*. 2012;18(19):2734–2757.
11. Marotti JD, Collins LC, Hu R, Tamimi RM. Estrogen receptor-β expression in invasive breast cancer in relation to molecular phenotype: results from the Nurses' Health Study. *Mod Pathol*. 2010;23(2):197–204.
12. Hanson IM. Mammalian homologues of the Drosophila eye specification genes. *Semin Cell Dev Biol*. 2001;12(6):475–484.
13. Rayapureddi JP, et al. Eyes absent represents a class of protein tyrosine phosphatases. *Nature*. 2003;426(6964):295–298.
14. Li X, et al. Eya protein phosphatase activity regulates Six1-Dach-Eya transcriptional effects in mammalian organogenesis. *Nature*. 2003;426(6964):247–254.
15. Tootle TL, et al. The transcription factor Eyes absent is a protein tyrosine phosphatase. *Nature*. 2003;426(6964):299–302.
16. Ohto H, et al. Cooperation of six and eya in activation of their target genes through nuclear translocation of Eya. *Mol Cell Biol*. 1999;19(10):6815–6824.
17. Xiong W, Dabbouseh NM, Rebay I. Interactions with the abelson tyrosine kinase reveal compartmentalization of eyes absent function between nucleus and cytoplasm. *Dev Cell*. 2009;16(2):271–279.
18. Okabe Y, Sano T, Nagata S. Regulation of the innate immune response by threonine-phosphatase of Eyes absent. *Nature*. 2009;460(7254):520–524.
19. Cook PJ, Ju BG, Telese F, Wang X, Glass CK, Rosenfeld MG. Tyrosine dephosphorylation of H2AX modulates apoptosis and survival decisions. *Nature*. 2009;458(7238):591–596.
20. Krishnan N, et al. Dephosphorylation of the C-terminal tyrosyl residue of the DNA damage-related histone H2A.X is mediated by the protein phosphatase eyes absent. *J Biol Chem*. 2009;284(24):16066–16070.
21. Zhang L, et al. Transcriptional coactivator Drosophila eyes absent homologue 2 is up-regulated in epithelial ovarian cancer and promotes tumor growth. *Cancer Res*. 2005;65(3):925–932.
22. Pandey RN, et al. The Eyes Absent phosphatase-transactivator proteins promote proliferation, transformation, migration, and invasion of tumor cells. *Oncogene*. 2010;29(25):3715–3722.
23. Farabaugh SM, Micalizzi DS, Jedlicka P, Zhao R, Ford HL. Eya2 is required to mediate the pro-metastatic functions of Six1 via the induction of TGF-β signaling, epithelial-mesenchymal transition, and cancer stem cell properties. *Oncogene*. 2012;31(5):552–562.
24. Colicelli J. ABL tyrosine kinases: evolution of function, regulation, and specificity. *Sci Signal*. 2010;3(139):re6.
25. Hunter T. Treatment for chronic myelogenous leukemia: the long road to imatinib. *J Clin Invest*. 2007;117(8):2036–2043.
26. Ganguly SS, Plattner R. Activation of abl family kinases in solid tumors. *Genes Cancer*. 2012; 3(5-6):414–425.
27. Srinivasan D, Sims JT, Plattner R. Aggressive breast cancer cells are dependent on activated Abl kinases for proliferation, anchorage-independent growth and survival. *Oncogene*. 2008;27(8):1095–1105.
28. Kiely PA, et al. Phosphorylation of RACK1 on tyrosine 52 by c-ABL is required for insulin-like growth factor I-mediated regulation of focal adhesion kinase. *J Biol Chem*. 2009;284(30):20263–20274.
29. Noren NK, Foos G, Hauser CA, Pasquale EB. The EphB4 receptor suppresses breast cancer cell tumorigenicity through an Abl-Crk pathway. *Nat Cell Biol*. 2006;8(8):815–825.
30. Allington TM, Galliher-Beckley AJ, Schiemann WP. Activated Abl kinase inhibits oncogenic transforming growth factor-β signaling and tumorigenesis in mammary tumors. *FASEB J*. 2009;23(12):4231–4243.
31. Cristofanilli M, et al. Imatinib mesylate (Gleevec) in advanced breast cancer-expressing C-Kit or PDGFR-β: clinical activity and biological correlations. *Ann Oncol*. 2008;19(10):1713–1719.
32. Yardley DA, et al. Phase II trial of docetaxal plus imatinib mesylate in the treatment of patients with metastatic breast cancer. *Clin Breast Cancer*. 2009;9(4):237–242.
33. Tsai KK, Yuan ZM. c-ABL stabilizes p73 by a phosphorylation-augmented interaction. *Cancer Res*. 2003;63(12):3418–3424.
34. Yang J, et al. Discovery and characterization of a cell-permeable, small-molecule c-ABL kinase activator that binds to the myristoyl binding site. *Chem Biol*. 2011;18(2):177–186.
35. Stuart JR, Kawai H, Tsai KK, Chuang EY, Yuan

ZM. c-ABL regulates early growth response protein (EGR1) in response to oxidative stress. *Oncogene*. 2005;24(55):8085–8092.
36. Ohtake F, et al. Modulation of oestrogen receptor signalling by association with the activated dioxin receptor. *Nature*. 2003;423(6939):545–550.
37. Bouchal J, Santer FR, Hoschele PP, Tomastikova E, Neuwirt H, Culig Z. Transcriptional coactivators p300 and CBP stimulate estrogen receptor-β signaling and regulate cellular events in prostate cancer. *Prostate*. 2011;71(4):431–437.
38. Metivier R, et al. Estrogen receptor-a directs ordered, cyclical, and combinatorial recruitment of cofactors on a natural target promoter. *Cell*. 2003;115(6):751–763.
39. Cheng L, et al. PES1 promotes breast cancer by differentially regulating ERα and ERβ. *J Clin Invest*. 2012;122(8):2857–2870.
40. Allington TM, Schiemann WP. The Cain and Abl of epithelial-mesenchymal transition and transforming growth factor-β in mammary epithelial cells. *Cells Tissues Organs*. 2011;193(1–2):98–113.
41. Tremblay GB, et al. Cloning, chromosomal localization, and functional analysis of the murine estrogen receptor β. *Mol Endocrinol*. 1997;11(3):353–365.
42. Tremblay A, Tremblay GB, Labrie F, Giguere V. Ligand-independent recruitment of SRC-1 to estrogen receptor β through phosphorylation of activation function AF-1. *Mol Cell*. 1999;3(4):513–519.
43. Picard N, et al. Phosphorylation of activation function-1 regulates proteasome-dependent nuclear mobility and E6-associated protein ubiquitin ligase recruitment to the estrogen receptor β. *Mol Endocrinol*. 2008;22(2):317–330.
44. Sanchez M, Picard N, Sauve K, Tremblay A. Challenging estrogen receptor β with phosphorylation. *Trends Endocrinol Metab*. 2010; 21(2):104–110.
45. Lam HM, et al. Phosphorylation of human estrogen receptor-beta at serine 105 inhibits breast cancer cell migration and invasion. *Mol Cell Endocrinol*. 2012;358(1):27–35.
46. Jackson RL, Greiwe JS, Schwen RJ. Emerging evidence of the health benefits of S-equol, an estrogen receptor β agonist. *Nutr Rev*. 2011;69(8):432–448.
47. Ishiwata N, Melby MK, Mizuno S, Watanabe S. New equol supplement for relieving menopausal symptoms: randomized, placebo-controlled trial of Japanese women. *Menopause*. 2009;16(1):141–148.
48. Krueger AB, et al. Identification of a selective small-molecule inhibitor series targeting the eyes absent 2 (Eya2) phosphatase activity. *J Biomol Screen*. 2012;18(1):85–96.
49. Zhang H, et al. Stimulatory cross-talk between NFAT3 and estrogen receptor in breast cancer cells. *J Biol Chem*. 2005;280(52):43188–43197.
50. Secreto FJ, Monroe DG, Dutta S, Ingle JN, Spelsberg TC. Estrogen receptor α/β isoforms, but not betacx, modulate unique patterns of gene expression and cell proliferation in Hs578T cells. *J Cell Biochem*. 2007;101(5):1125–1147.
51. Aiyar SE, et al. Attenuation of estrogen receptor α-mediated transcription through estrogen-stimulated recruitment of a negative elongation factor. *Genes Dev*. 2004;18(17):2134–2146.
52. Hu Y-F, Miyake T, Ye Q, Li R. Characterization of a novel trans-activation domain of BRCA1 that functions in concert with the BRCA1 C-terminal (BRCT) domain. *J Biol Chem*. 2000;275(52):40910–40915.
53. Ding N, et al. Mediator links epigenetic silencing of neuronal gene expression with x-linked mental retardation. *Mol Cell*. 2008;31(3):347–359.
54. Ding L, et al. Human four-and-a-half LIM family members suppress tumor cell growth through a TGF-β-like signaling pathway. *J Clin Invest*. 2009;119(2):349–361.